Supporting Information

Label-free Mapping of Cetuximab in Multi-layered Tumor Oral Mucosa models by Atomic Force-Microscopy-based Infrared Spectroscopy

Gregor Germer[a,+], Leonie Schwartze[b,+], Jill García-Miller[b], Roberta Balansin-Rigon[b,c], Lucie J. Groth[a], Isabel Rühl[a], Piotr Patoka[a], Christian Zoschke[b,d,*], Eckart Rühl[a,*]

[a] Physical Chemistry, Freie Universität Berlin, Arnimallee 22, 14195 Berlin, Germany

[b] Institute of Pharmacy, Freie Universität Berlin, Königin-Luise Str. 2+4, 14195 Berlin, Germany

[c] School of Pharmaceutical Sciences, University of Campinas, R. Candido Portinari, 200 - Cidade Universitária, Campinas - SP, 13083-871, Brazil

[d] Department of Veterinary Medicines, Federal Office of Consumer Protection and Food Safety, Gerichtstr. 49, 13347 Berlin, Germany

[+] contributed equally/shared 1st authorship

* corresponding authors

1. Cross Sensitivities of Cetuximab Probing in untreated TOM Models

The morphology of the untreated TOM model (Figure S1) is similar to the treated ones shown in Figures 1 and S12. Data reduction was performed as described in the main text to determine the background signal for cetuximab detection and to avoid cross sensitivities of the cetuximab-treated samples, where two different analysis approaches are used: linear combination modeling (labeled 1) and singular value decomposition-based PCA analysis (labeled 2). Selected locations A, B, and C are superimposed to results on the spatial distribution of the spectral signature of cetuximab in Figure S2. The background signal in the untreated TOM models is slightly lower than that of cetuximab in the cetuximab-treated samples, where in Figure S2 for the tumor regions B and C a background level of 0.15 was used and there is only spurious signal exceeding this value. Depending on the analyzed location A, B, and C there is some structured signal of cetuximab, which corresponds to cross-sensitivities, especially for the region of lamina propria (location A). Figures S3, S4, and S5 show the result of the analysis of the other species considered by both analysis approaches at the locations A, B, and C. Most clearly at location C, the contribution from reference 1 (Figure 2(b)) and principal component 1 (Figure 3(b)) shown in Figure S5(a) and (g), respectively, is mostly found in the cytosol of the cells with a distinct drop in intensity at the nuclear membrane. It is similar in spatial distribution as the cetuximab distribution shown

in Figures 4 and 6, which underscores evidence for cross sensitivities in the tumor epithelium regime. The spatial distribution of the spectral component of reference cell 2 region shows no distinct localization (Figure S5(b)), whereas PBS is strongly localized near the cell membranes (Figure S5(c)). The cryo medium and the silicon substrate show no spatially distinct distribution, as can be expected for these spectral channels (Figure S5(d) and (e)). Finally, the offset is also broadly distributed with minima in the cell membranes (see Figure S5(f)). The spatial distribution of principal component 1 (Figure S5(g)) shown almost an identical distribution as that of reference cell 1 (cf. Figure S5(a)). The spatial distribution of the principal components 2-5 (Figure S5(h)-(k)) is less clear than that of the reference spectra and underscores their limited physical relevance. Finally, the offset component (Figure S5(l)) shows slightly enhanced contributions in the cytosol of cells, which is opposite to the offset resulting from linear combination modeling.

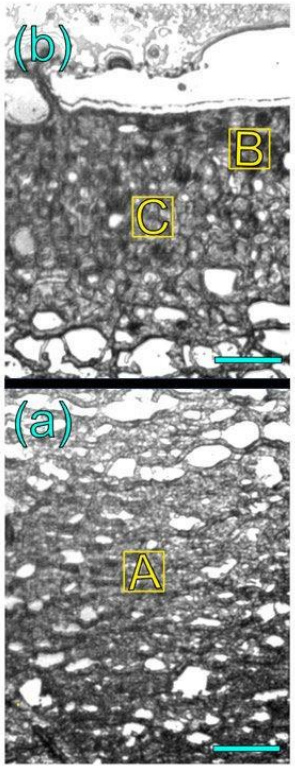

Figure S1: Optical micrographs of two untreated TOM models: (a) lamina propria and (b) tumor epithelium with three selected cell locations (A, B, and C). Scale bars (light blue): 50 µm.

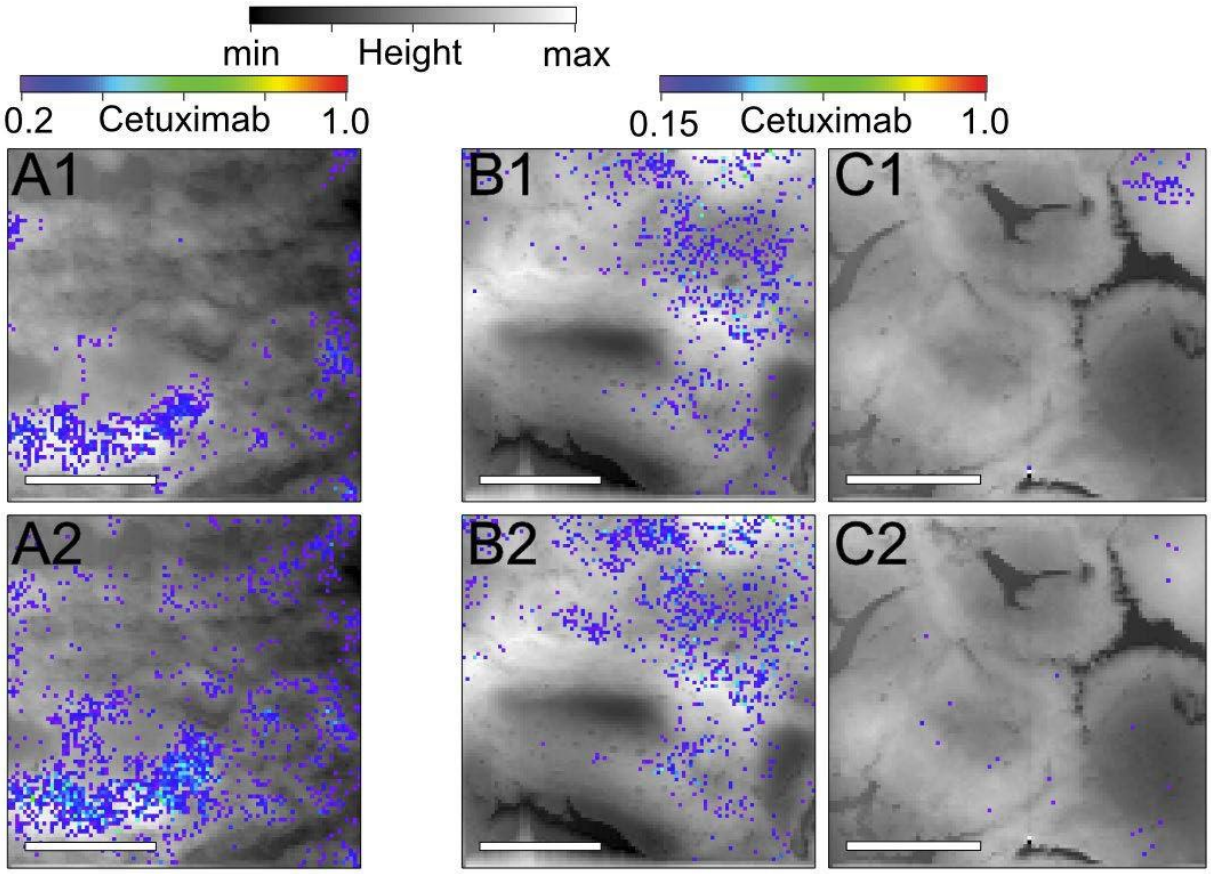

Figure S2: Distribution of the cetuximab contribution in an untreated TOM model sample at three locations (A, B, and C) derived from linear combination modeling of reference spectra (labeled 1) and singular value decomposition-based PCA analysis (labeled 2) for determining cross sensitivities. The scale bar corresponds to 10 µm.

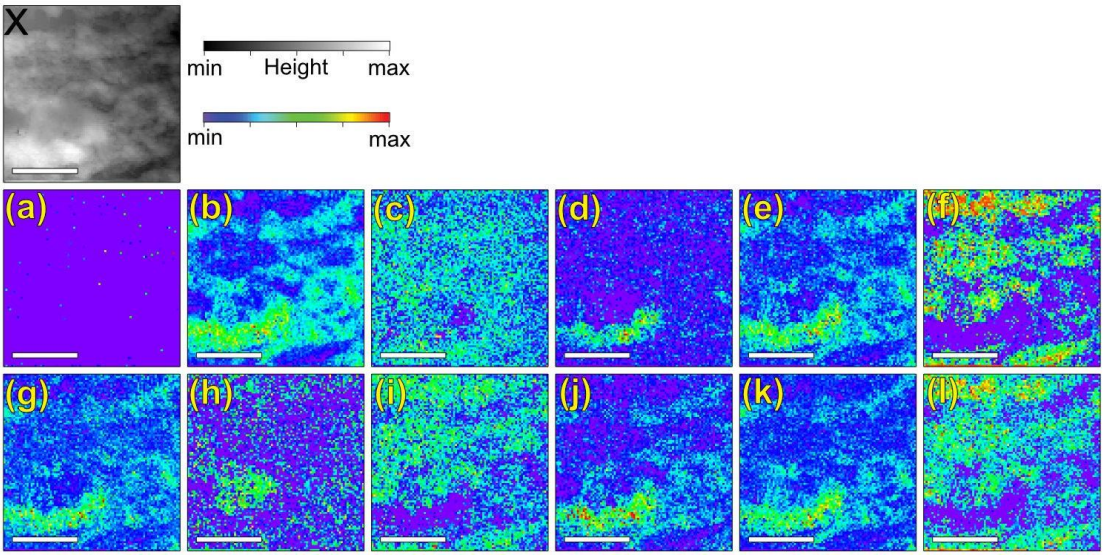

Figure S3: Lamina propria of an untreated TOM model at location A (lamina propria) (Figure S1 and S2(A)): Top row AFM topography height image (X). Middle row: Spatial distribution of the experimental reference samples expressed by the local abundance aa_{ii} (see Figure 2) as derived from linear combination modeling of reference spectra: (a) reference lamina propria 1 region, (b) reference lamina propria 2 region, (c) PBS, (d) PEG-based cryo medium, (e) silicon substrate, and (f) offset. Bottom row: Spatial distribution of the principal components 1 - 5 (left to right) derived from singular value decomposition-based PCA analysis labeled (g) - (k) and (l) offset (cf. Figure 3). The scale bar corresponds to 10 µm.

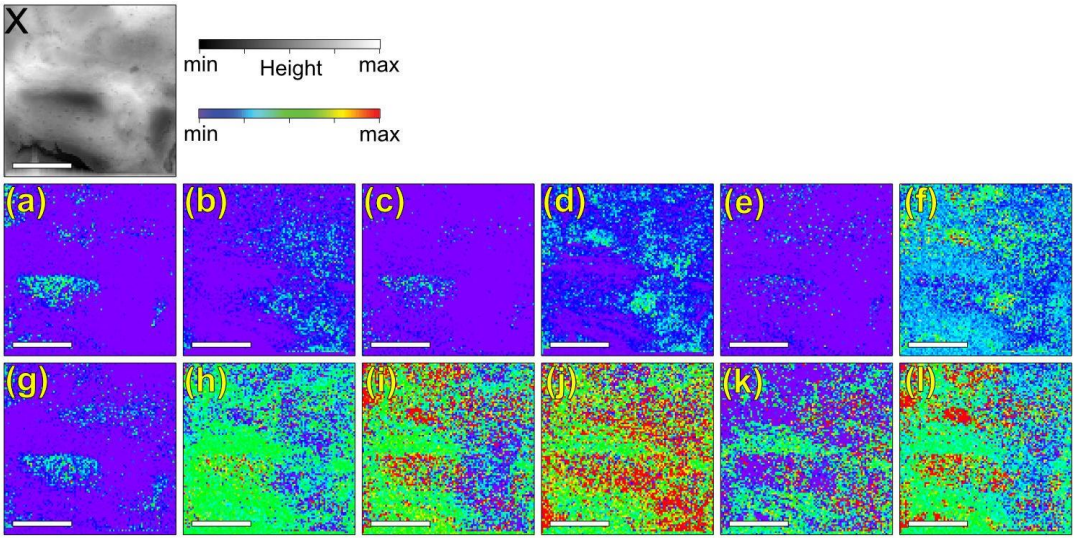

Figure S4: Tumor epithelium of an untreated TOM model at location B (Figure S1 and S2(B)): Top row AFM topography height image (X). Middle row: Spatial distribution of the experimental reference samples expressed by the local abundance aa_{ii} (see Figure 2) as derived from linear combination modeling of reference spectra: (a) reference lamina propria 1 region, (b) reference lamina propria 2 region, (c) PBS, (d) PEG-based cryo medium, (e) silicon substrate, and (f) offset. Bottom row: Spatial distribution of the principal components 1 - 5 (left to right) derived from singular value decomposition-based PCA analysis labeled (g) - (k) and (l) offset (cf. Figure 3). The scale bar corresponds to 10 µm.

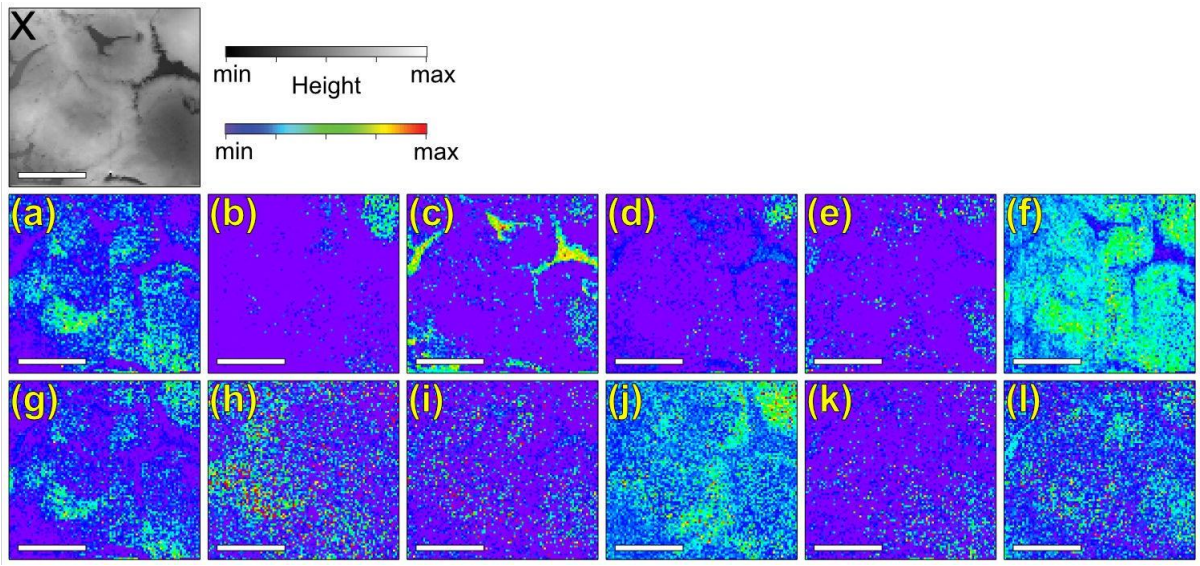

Figure S5: Tumor epithelium of an untreated TOM model at location C (Figure S1 and S2(C)): Top row AFM topography height image (X). Middle row: Spatial distribution of the experimental reference samples expressed by the local abundance a_{ij} (see Figure 2) as derived from linear combination modeling of reference spectra: (a) reference lamina propria 1 region, (b) reference lamina propria 2 region, (c) PBS, (d) PEG-based cryo medium, (e) silicon substrate, and (f) offset. Bottom row: Spatial distribution of the principal components 1 - 5 (left to right) derived from singular value decomposition-based PCA analysis labeled (g) - (k) and (l) offset (cf. Figure 3). The scale bar corresponds to 10 µm.

2. Principal Components in the Lamina Propria Region

Studies on the local drug distribution require separate locations where the principal component analysis was performed (see Figure 3). The data shown in Figure 3 were taken at the tumor cells C, D, and E of Figure 1. As an alternative, principal components were also derived from the lamina propria regions A and B (see Figure 1). The corresponding principal components are shown in Figure S6. The results from Figure S6 are used for determining the distributions and local concentrations of cetuximab in lamina propria at the locations A and B of Figure 1, as shown in Figure 4 at the locations A2 and B2.

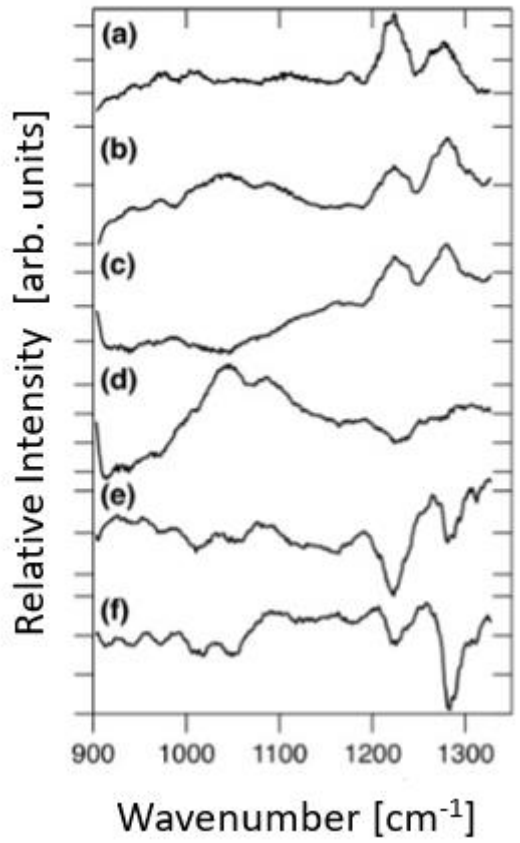

Figure S6: (a) AFM-IR reference spectrum of cetuximab; results from a principal component analysis of the lamina propria region: (b) component 1 (average spectrum of the region); (c) component 2; (d) component 3; (e) component 4; (f) component 5, used as input for singular value decomposition-based PCA analysis of the lamina propria region (see Figure 4 analysis of regions A2 and B2).

3. Analysis of the Topically Treated TOM Model

The spatial distributions and local concentrations of the other spectral components (cf. Figure 2 and 3) besides cetuximab (see Figures 4 and 5) were determined for the topically treated TOM model at the locations A – E. These are: (i) an AFM height image of the selected locations (cf. top row of Figures S7 - S11); (ii) the spatial distribution of the other analyzed spectral components shown in Figure 2, as derived from linear combination modeling of reference spectra, shown in the middle rows of Figures S7 - S11; and (iii) the bottom rows of Figures S7 - S11 indicate the spatial distributions of singular value decomposition-based PCA analysis depicted in Figure 3 and S6, respectively. Most clear are the images and spatial distributions at the locations C and D, corresponding to tumor epithelium (cf. Figures S9 and S10). Those at the other locations (A, B: lamina propria, E: tumor epithelium) are somewhat blurred and do not allow for correlating the cellular morphology with the observed spatial distributions. Linear combination modeling of reference spectra yields the following results: The contribution of reference tumor cell 1 region is mostly found in the cytosol of the cells (see Figures S9(a) and S10(a)), whereas the reference tumor cell 2 contribution shows only low intensity (see Figures S9(b) and S10(b)). Thus, the spectral distribution at location 1 is most relevant for the sample under study. PBS is mostly found in tumor cells in the cytoplasm and not in membranes (see Figures S9(c) and S10(c)) and not in the nucleus (Figure S9(c)). The cryo medium (see Figure S9(d) and S10(d)) shows only weak abundance. The silicon substrate (see Figure S9(e) and S10(e)) mostly occurs in regions of low height and at the cell nucleus (cf. Figure 9(e)), which hints a different composition of the nucleus that favors detection of the substrate. The spatial distributions of the principal components used for singular value decomposition-based PCA analysis (cf. Figure 3 and S6) show for some components (especially 2, 3, 5) high intensity near the cell membranes (cf. Figures S9(h), (i), (k) and 10 (h), (i), (k)).

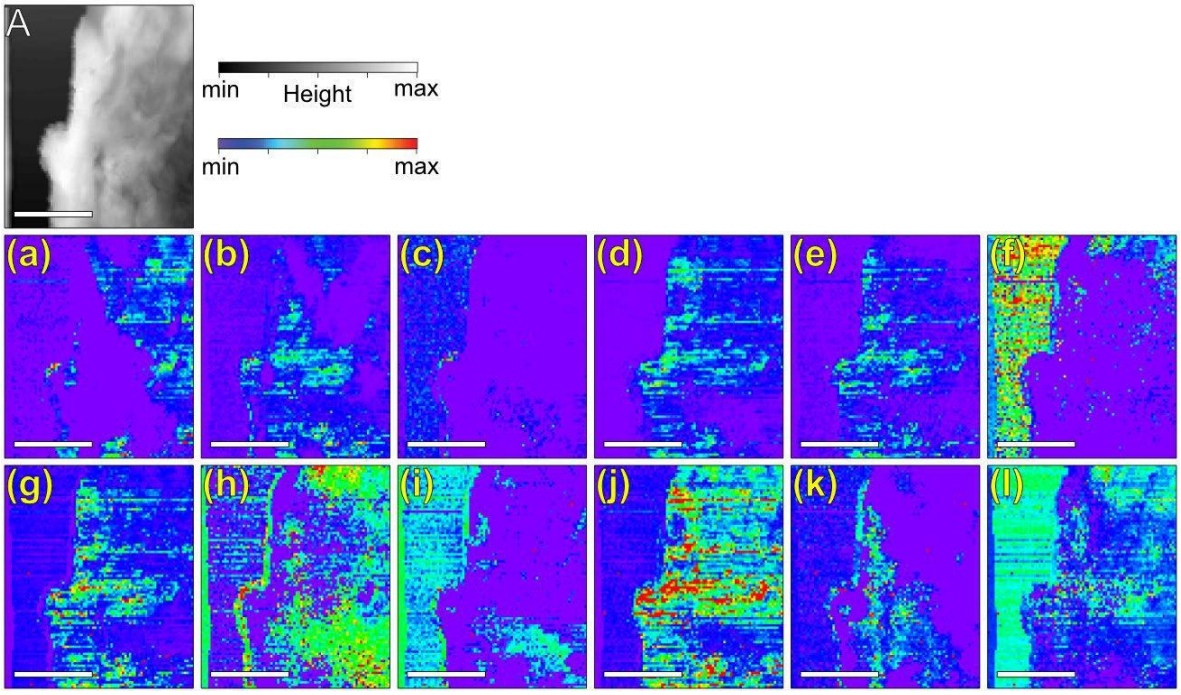

Figure S7: Spatial distribution of spectral components in a topically treated TOM model (Lamina propria location A, see Figures 1 and 4). Top row: AFM topography height image. Middle row: Spatial distribution derived from linear combination modeling of reference spectra expressed by the local abundance aa_{ij} (see Figure 2): (a) lamina propria region 1, (b) lamina propria region 2, (c) PBS, (d) PEG-based cryo medium, (e) silicon substrate, and (f) offset. Bottom row (g) - (k): Spatial distribution derived from singular value decomposition-based PCA analysis of components 1 - 5 (left to right) (cf. Figure S6). (l) corresponds to an offset. Scale bar: 10 µm.

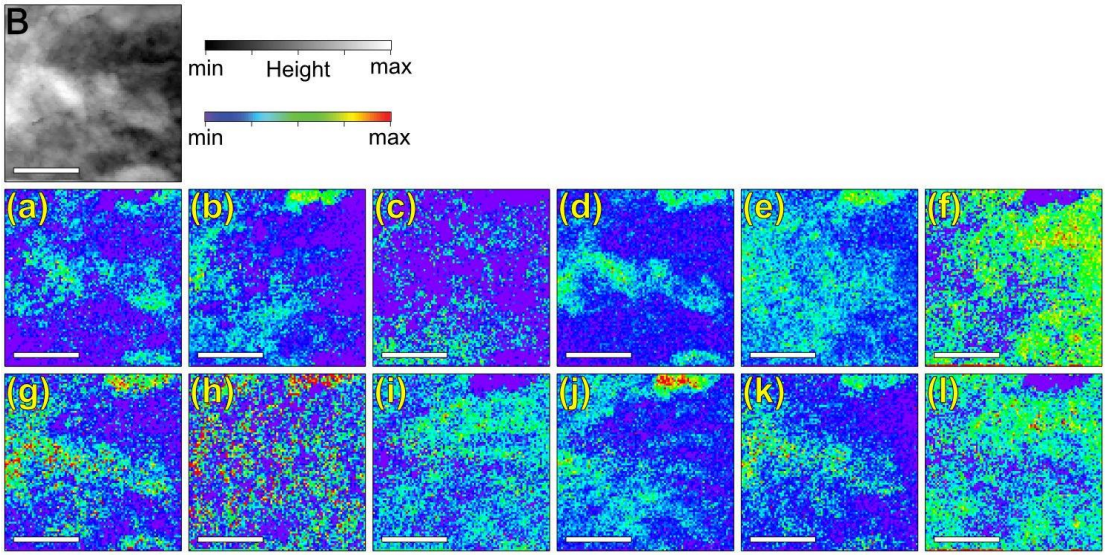

Figure S8: Spatial distribution of spectral components in a topically treated TOM model (Lamina propria location B, see Figures 1 and 4). Top row: AFM topography height image. Middle row: Spatial distribution derived from linear combination modeling of reference spectra expressed by the local abundance aa_{ii} (see Figure 2): (a) lamina propria region 1, (b) lamina propria region 2, (c) PBS, (d) PEG-based cryo medium, (e) silicon substrate, and (f) offset. Bottom row (g) - (k): Spatial distribution derived from singular value decomposition-based PCA analysis of components 1 - 5 (left to right) (cf. Figure S6). (l) corresponds to an offset. Scale bar: 10 µm.

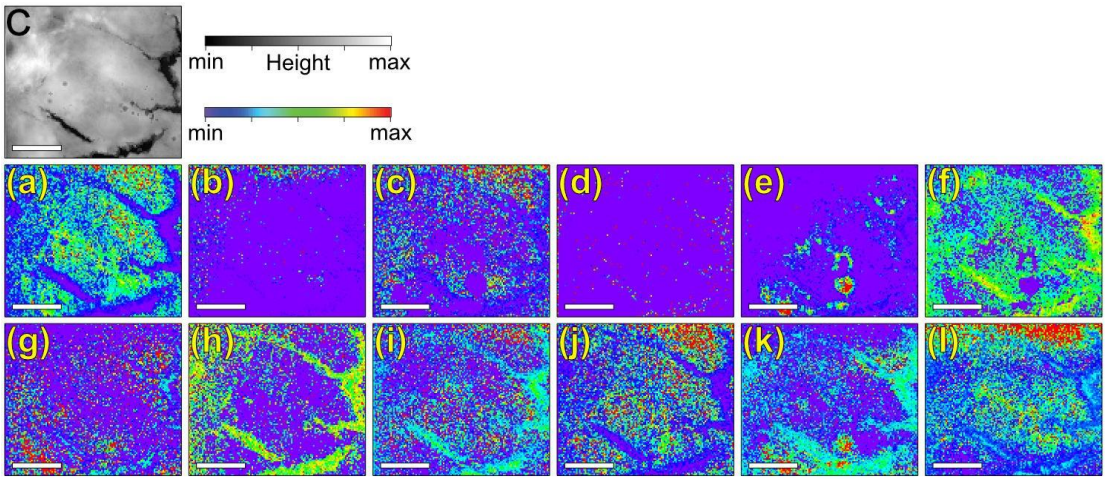

Figure S9: Spatial distribution of spectral components in a topically treated TOM model (tumor epithelium, location C, see Figures 1 and 4). Top row: AFM topography height image. Middle row: Spatial distribution derived from linear combination modeling of reference spectra expressed by the local abundance aa_{ii} (see Figure 2): (a) tumor cell region 1, (b) tumor cell region 2, (c) PBS, (d) PEG-based cryo medium, (e) silicon substrate, and (f) offset. Bottom row (g) - (k): Spatial distribution derived from singular value decomposition-based PCA analysis of components 1 - 5 (left to right) (cf. Figure 3). (l) corresponds to an offset. Scale bar: 10 µm.

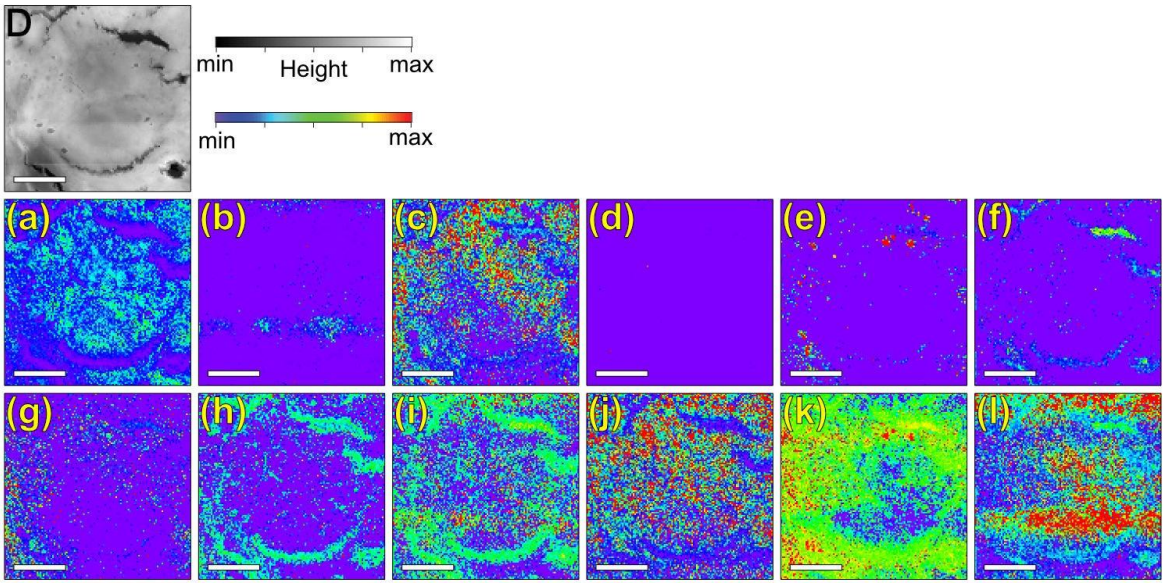

Figure S10: Spatial distribution of spectral components in a topically treated TOM model (tumor epithelium, location D, see Figures 1 and 4). Top row: AFM topography height image. Middle row: Spatial distribution derived from linear combination modeling of reference spectra expressed by the local abundance aa_{ii} (see Figure 2): (a) tumor cell region 1, (b) tumor cell region 2, (c) PBS, (d) PEG-based cryo medium, (e) silicon substrate, and (f) offset. Bottom row (g) - (k): Spatial distribution derived from singular value decomposition-based PCA analysis of components 1 - 5 (left to right) (cf. Figure 3). (l) corresponds to an offset. Scale bar: 10 µm.

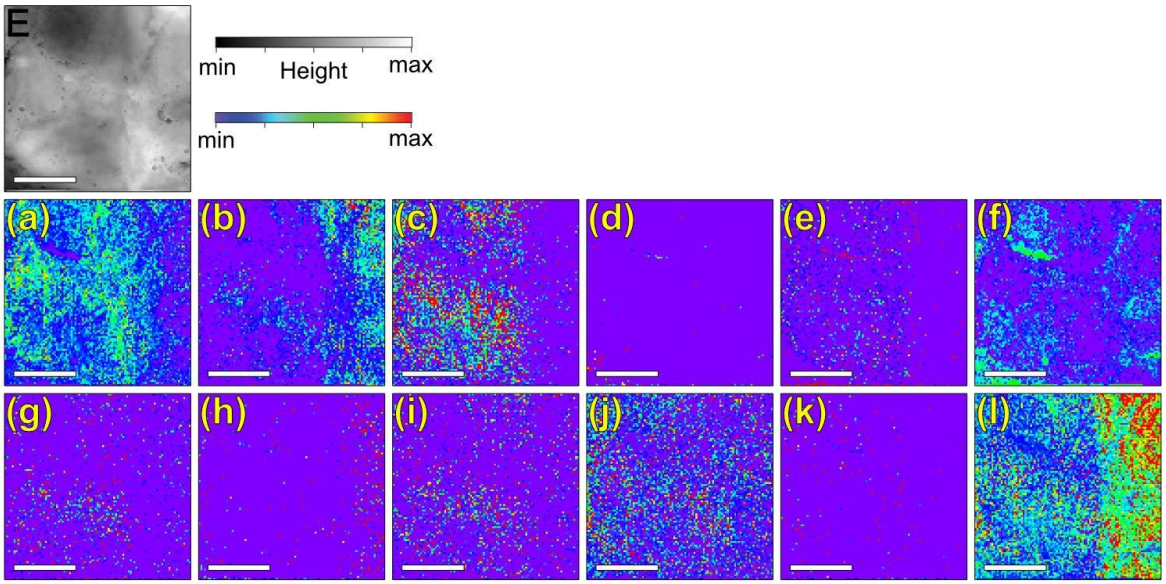

Figure S11: Spatial distribution of spectral components in a topically treated TOM model (tumor epithelium, location E, see Figures 1 and 4). Top row: AFM topography height image. Middle row: Spatial distribution derived from linear combination modeling of reference spectra expressed by the local abundance aa_{ii} (see Figure 2): (a) tumor cell region 1, (b) tumor cell region 2, (c) PBS, (d) PEG-based cryo medium, (e) silicon substrate, and (f) offset. Bottom row (g) - (k): Spatial distribution derived from singular value decomposition-based PCA analysis of components 1 - 5 (left to right) (cf. Figure 3). (l) corresponds to an offset. Scale bar: 10 µm.

4. Analysis of the Systemically Treated TOM Model

A systemically treated TOM model was included into the study, where the drug was contained in the model medium, resulting in a drug application from the lamina propria side of the samples. Figure S12 shows this sample along with four locations that were investigated in greater detail. Note that the surface of the sample is in Figure S12 on the right-hand side and the cell medium is on the left-hand side. These locations labeled A – D indicate, as based on the same analysis that was applied to the topically treated sample, that cetuximab can be found at all four locations. Figures S13 - S16 show the other spatial distributions of the species besides cetuximab included in Figure 2. The morphology of the cells can be most clearly correlated with the spatial distribution of the analyzed species at location D (cf. Figures S12 and S16). Here, the spatial distribution of the tumor reference cell 1 component is located inside the cells, but not near the membranes, whereas the other tumor reference cell 2 shows a faint signal near the cell membrane, indicating that this component has no relevance for the data analysis. This is also true for the spatial distribution of PBS and the cryo medium (Figure S16(c) and (d)). Moreover, there is high abundance inside tumor cells for the silicon substrate (Figure S16(e)), which is not correlated to the thickness of the sample and is different for the topically treated samples (see above).

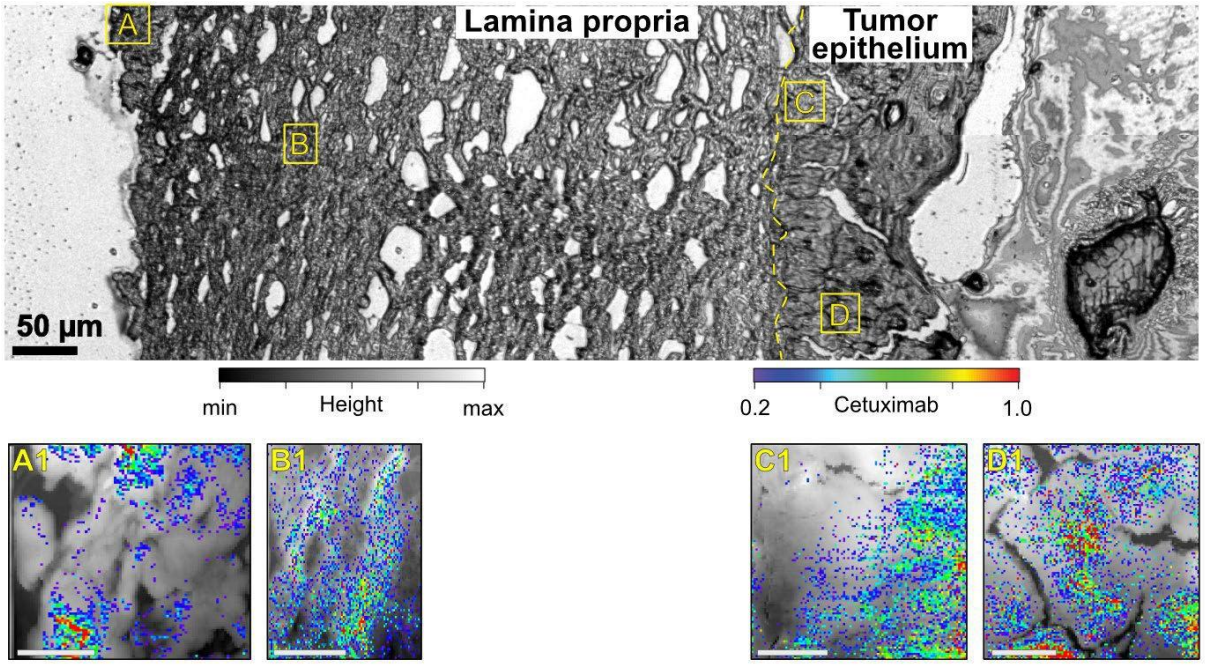

Figure S12: Systemically treated TOM model. Top row: Optical micrographs of the systemically treated TOM model. The investigated regions are labeled by yellow squares (A, B: lamina propria and C, D: tumor epithelium). Scale bar in the top row: 50 µm. Bottom row: AFM height channel signal presented in a grey scale recorded at two locations in the lamina propria (A1 and B1), and the tumor epithelium (C1 and D1). The color-coded intensity represents the local distribution of cetuximab based on linear combination modeling of reference spectra (cf. Figure 2). Scale bar in the bottom row: 10 µm. See text for further details.

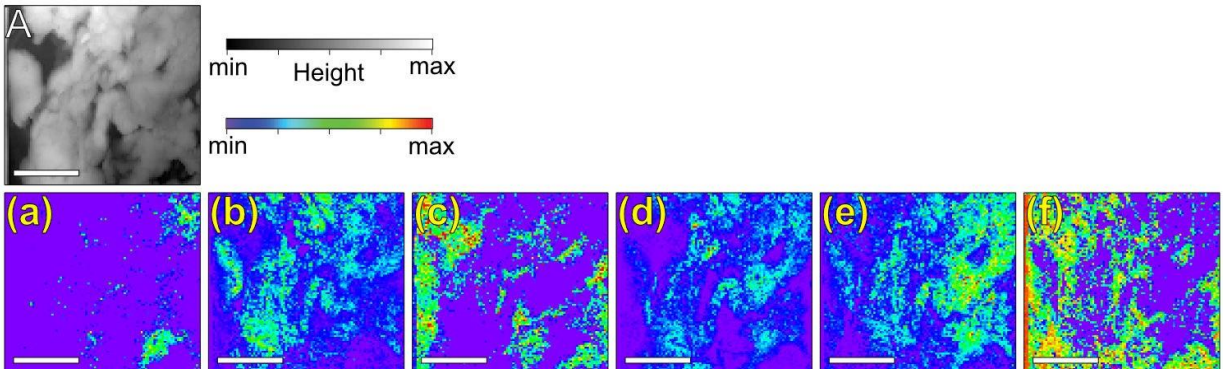

Figure S13: Lamina propria region A of the systemically treated TOM model (see Figure S12). Top row: AFM topography height image; Bottom: Spatial distribution of the experimental reference samples expressed by the local abundance a_{ij} as derived from linear combination modeling (see Figure 2): (a) lamina propria region 1, (b) lamina propria region 2, (c) PBS, (d) PEG-based cryo medium, (e) silicon substrate, and (f) offset. The scale bar: 10 µm.

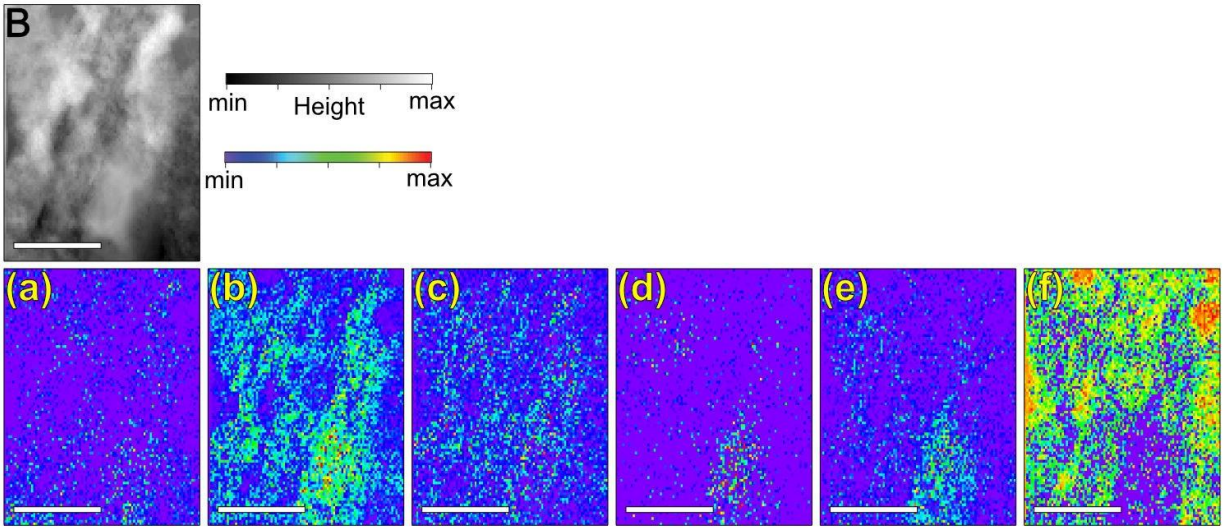

Figure S14: Lamina propria region B of the systemically treated TOM model (see Figure S12). Top row: AFM topography height image; Bottom: Spatial distribution of the experimental reference samples expressed by the local abundance a_{ij} as derived from linear combination modeling (see Figure 2): (a) lamina propria region 1, (b) lamina propria region 2, (c) PBS, (d) PEG-based cryo medium, (e) silicon substrate, and (f) offset. The scale bar: 10 µm.

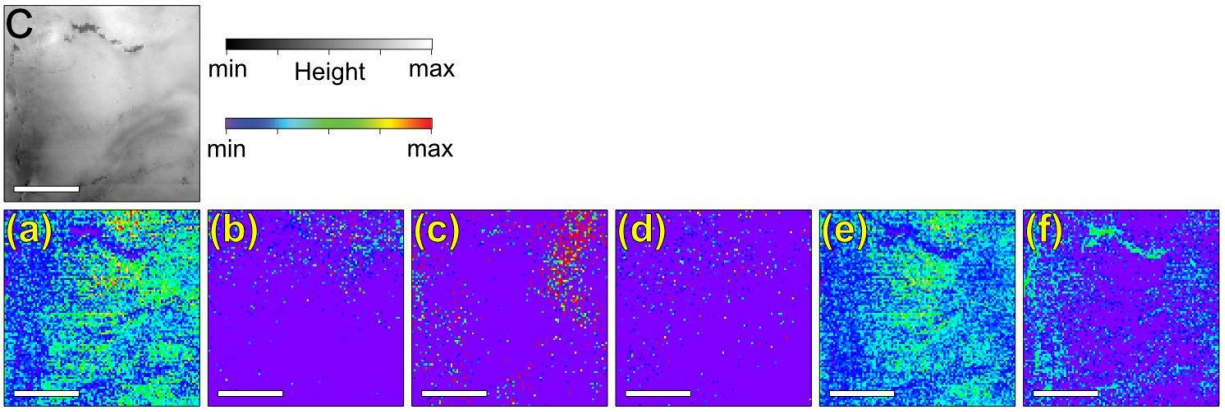

Figure S15: Tumor epithelium region C of the systemically treated TOM model (see Figure S12). Top row: AFM topography height image; Bottom: Spatial distribution of the experimental reference samples expressed by the local abundance aa_{ij} as derived from linear combination modeling (see Figure 2): (a) tumor reference cell 1, (b) tumor reference cell 2, (c) PBS, (d) PEG-based cryo medium, (e) silicon substrate, and (f) offset. The scale bar: 10 µm.

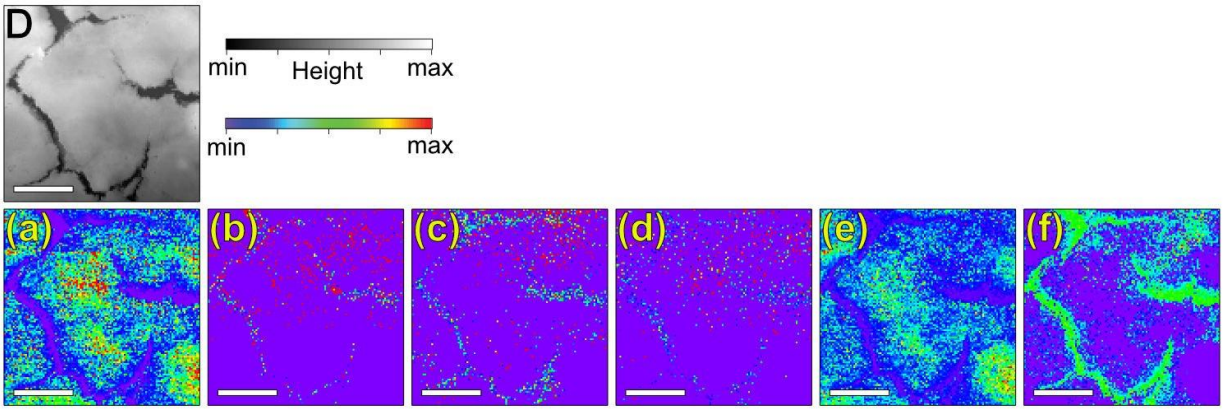

Figure S16: Tumor epithelium region D of the systemically treated TOM model (see Figure S12). Top row: AFM topography height image; Bottom: Spatial distribution of the experimental reference samples expressed by the local abundance aa_{ij} as derived from linear combination modeling (see Figure 2): (a) tumor reference cell 1, (b) tumor reference cell 2, (c) PBS, (d) PEG-based cryo medium, (e) silicon substrate, and (f) offset. The scale bar: 10 µm.

5. High Spatial Resolution Studies

High spatial resolution studies provide further insights into the spatial distribution of cetuximab in cells after topical treatment, as shown in Figure 6. Figure S17 shows the spatial distribution of the other species that were analyzed by linear combination modeling of reference spectra (middle row). Most species show no distinct spatial distributions that can be related to the nuclear membrane, only the tumor reference cell 2 component (Figure S17(b)) and the offset (Figure S17(f)) show some distinct features which can be correlated with the nuclear membrane. However, none of them shows the same characteristics as that of cetuximab. The same conclusions can be drawn from the results derived from singular value decomposition-based PCA analysis (Figure S17(g) – (l)).

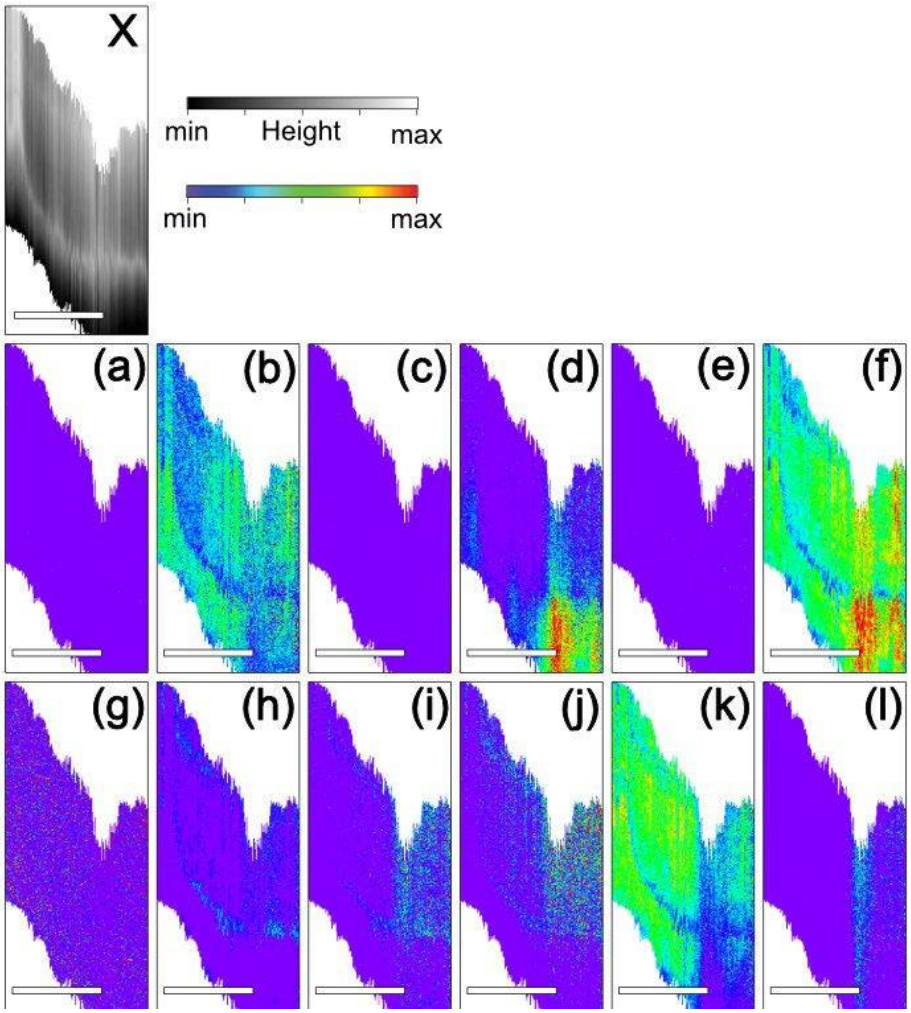

Figure S17: High-resolution scans of the nuclear membrane. The scanned region is marked in Figure 6 by a red rectangle. Top (X): AFM topography height image. Middle row: Spatial distributions expressed by the local abundance aa_{ii} as derived from linear combination modeling of reference spectra (see Figure 2): (a) tumor reference cell 1, (b) tumor reference cell 2 (c) PBS, (d) PEG-based cryo medium, (e) silicon substrate, and (f) offset. Bottom row: Results from singular value decomposition-based PCA analysis, where (g) – (k) indicate the spatial distributions of the principal components 1 - 5 (left to right) (cf. Figure 3 and S6); (l) corresponds to an offset. Scale bar: 0.5 µm.